Non-Gaussian stochastic dynamics of spins and oscillators: A continuous-time random walk approach

Daniel M. Packwood* and Yoshitaka Tanimura
Department of Chemistry, Graduate School of Science, Kyoto University, Kyoto 606-8502, Japan
(Received 17 May 2011; revised manuscript received 6 October 2011; published 7 December 2011)

We consider separately a spin and an oscillator that are coupled to their environment. After a finite interval of random length, the state of the environment changes, and each change causes a random change in the resonance frequency of the spin or vibrational frequency of the oscillator. Mathematically, the evolution of these frequencies is described by a continuous-time random walk. Physically, the stochastic dynamics can be understood as non-Gaussian because the frequency of the system and state of the environment change on comparable time scales. These dynamics are also nonstationary, and so might apply to a nonequilibrium environment. The resonance and vibrational spectra of the spin and oscillator, as well as the ensemble-averaged displacement of the oscillator, are investigated in detail. We observe some distinct non-Gaussian features of the dynamics, such as the narrow, leptokurtic shape of the resonance spectrum of the spin and beating of the average oscillator displacement. The convergence to Gaussian dynamics as changes in the environment occur with increasing frequency is also considered. Among other results, we observe narrowing of the resonance and vibrational lines in the Gaussian limit due to a weakening of the system-environment interaction.

DOI: 10.1103/PhysRevE.84.061111 PACS number(s): 05.40.Ca, 05.40.Fb, 02.50.Ey

I. INTRODUCTION

Stochastic processes are versatile ways of describing the effect of a random, many-body environment on the time evolution of a system. They serve as projections of the environment's motion on the system, and appear in the equations of motion for the system as either parameters or forces. Aside from massive numerical simulations, stochastic processes cannot in general be derived from detailed microscopic models for the environment, and so the choice of a specific process for a particular problem is subjective. Gaussian stochastic processes, in which the probability distribution function for the process at all times is given by Gaussian (normal) distribution, are popular choices for a variety of problems since their well-developed mathematical theory allows for reasonable handling [1,2]. Gaussian processes are applicable whenever the time scale of the system's motion is considerably longer than the time scale of the motion of the environment degrees of freedom. This interpretation follows from the central limit theorem, which states that the sum of independent and identically distributed random variables converges to a Gaussian random variable as the number of terms in the sum becomes infinite.

If a system's motion is on a time scale much larger than that its surroundings, then each individual system-environment degree of freedom interaction can only ever have a very small influence on the system's trajectory. In Gaussian stochastic models, this requirement appears in a variety of ways. For example, in the usual theory of Brownian motion the Brownian particle is assumed to be considerably more massive than the surrounding fluid. However, chemical problems involve molecule-molecule interactions, and in many cases the molecules of the environment and the system do not differ enough for the individual system-environment interactions to be as weak as a Gaussian theory demands. It is therefore not too surprising that sensitive experimental techniques such as nonlinear spectroscopies have detected non-Gaussian dynamics in several condensed phase systems. For example, Steinel *et al.* found that it is not possible to analyze correlation spectra of the O-D stretch of HOD if one assumes Gaussian interactions between the O-D oscillator and surrounding aqueous solvent molecules [3]. An experimental and computational study by Jansen *et al.* showed that Gaussian frequency fluctuations of an O-H stretch of water in acetonitrile do not account for differences observed in dephasing of the symmetric and asymmetric modes [4]. Further examples are discussed by Roy *et al.* [5]. This paper is concerned with the stochastic dynamics of systems whose motions have time scales comparable to those of the surrounding degrees of freedom, where one cannot assume Gaussian processes or apply methodologies based on Gaussian processes such as the cumulant expansion technique. We will offer a description of these non-Gaussian dynamics, and look at how these dynamics evolve into Gaussian dynamics in particular limits.

Before elaborating further on our own ideas, we point out that there is currently a large interest in non-Gaussian noises among the physics community. Baura *et al.* studied the escape rate of a particle from a metastable state subject to non-Gaussian noises defined by a type of Langevin equation [6]. Milotti has shown that non-Gaussianity arises very easily when analyzing data collected from relatively small samples using statistical estimators that are asymptotically Gaussian [7]. Non-Gaussian noises in semiconductors were investigated theoretically by Melkonyan using the idea that non-Gaussianity arises when only a few charge carriers participate in forming the noise on the time scale of acquiring a sample [8]. Augello *et al.* looked at the role of non-Gaussian noise in Josephson junctions using various examples of non-Gaussian distributions supplied by the probability literature [9]. Via first-principles theory, Danon and Brouwer investigated non-Gaussian distributions of the persistent current around thin conducting ring structures penetrated by a magnetic field [10]. A molecular dynamics simulation by Shin *et al.* looked at

*packwood@kuchem.kyoto-u.ac.jp

non-Gaussianity in the fluctuating force on Brownian particles of very small diameters [11]. In quite a different study, d'Onofrio and Gandolfi theoretically studied the resistance of tumor cells to drugs due to "noise-induced transitions," i.e., a stochastic interplay between various biological factors that leads to a resistance enhancement [12]. This study also defined the non-Gaussian noise using various types of Langevin equations. Each of these studies was published within the last two years. From this quick survey of the literature, it is nonetheless clear that there are no standard physical concepts associated with non-Gaussianity like we have for Gaussianity. A goal of this paper is to encourage developments in this direction.

This paper will consider separately a spin and an oscillator system coupled to environment degrees of freedom. In both cases, the underlying stochastic process works out to be a special case of a continuous-time random walk (CTRW), and is non-Gaussian in the sense that the time scale of the surroundings and system are assumed to be comparable. The spin model might be interpreted as a chromophore molecule in a host molecular crystal [13,14], or a solute molecule in a dipolar solvent [15–17]. We might regard the oscillator model as a model for the vibrational dephasing of a diatomic molecule in a diatomic solvent. An example is provided by HF liquids, in which the vibrational frequency of HF molecules changes in time due to the formation and deformation of the hydrogen coupling between the HF molecules [18]. Because we are considering a single spin or a single oscillator in contact with its environment, these can be regarded as models for single molecule trajectories. Explicit stochastic models for situations involving comparable system-environment time scales have been studied for many years (see, for example, [19]), several of which are reviewed in monograph by Dattagupta [20]. However, the CTRW treatment that we use has some differences. The non-Gaussian emphasis of this paper is because the CTRW has a well-defined Gaussian limit, as is necessary for a model of non-Gaussianity to be consistent with Gaussian models. In addition, the CTRW can be expressed in terms of sums of independent and identically distributed random variables. In many cases this will allow us to decompose our results into separate Gaussian and non-Gaussian contributions and to identify when a particular contribution can be neglected. Sums of independent and identically distributed random variables have a significant presence in the mathematical statistics literature (see, for example, [21]). Another difference from the above processes is that the CTRW that we use is nonstationary. The model is therefore relevant to a molecule in an environment that has been brought out of equilibrium by an external influence.

The single molecule CTRW approach therefore affords insights that compliment results from other theories [19–22]. Below we show beating behavior of the trajectory-averaged oscillator displacement as it relaxes from its initial value to its equilibrium value. Moreover, the form of the renormalization will make it clear how the system-environment interaction becomes particularly weak in approaching the Gaussian limit, providing physical insights into the narrowing phenomenon.

Section II constructs the stochastic process that will be used for the spin and oscillator models and establishes some of its statistical properties. The dynamics of the oscillator and the spectral lines of the central spin and the oscillator are investigated in Secs. III and IV gives some final remarks.

II. CONTINUOUS-TIME RANDOM WALK FREQUENCY MODULATION PROCESS

We consider two different problems. The first is an energy-fluctuating spin model, in which a spin (main system) is coupled to a large number of other spins (the environment). The fluctuations are due to random couplings to new spins or random decouplings from old spins. The second one is a frequency fluctuating oscillator model, in which the frequency of an oscillator (main system) fluctuates due to successive, random interactions with other oscillators (environment). The following will employ fixed initial conditions for the frequency of the spin and oscillator systems. This means that we are either preparing the systems in well-defined states and then introducing them to the environment, or waiting for the system to enter into a particular state before we start recording its trajectory. This might correspond to an idealized single-molecule experiment. Throughout the following, random variables and stochastic processes are denoted by capital italic Roman letters. A subscript t denotes the value of the stochastic process at time t. Expected values and variances will be denoted by $E()$ and var(), respectively.

In both cases, starting from time 0 we suppose that the main system stays in its initial state up to a random time U_1, where the state of the interacting environmental molecules change (i.e., a new spin couples to or an old spin decouples from the central spin, or the current environment oscillator decouples from the oscillator and a different one couples to it). The main system stays in this new arrangement of the environment molecules up to another random time U_2, when the environment undergoes another such change, then stays in this arrangement up to a random time U_3, and so on. The stochastic dynamics described by these models can be regarded as non-Gaussian. For the spin model, the resonance frequency of the central spin can change on a time scale comparable to changes in the state of the environment, and for the oscillator model the vibrational frequency of the central oscillator can be comparable to the frequency of new interactions with environment oscillators.

Three important assumptions will be made for both models. Let $K_1 = U_1, K_2 = U_2 - U_1, \ldots$ be the durations over which the main system remains a particular arrangement of the environment molecules. We will suppose that these durations are independent of one another and have the same probability distribution. If $1/\lambda$ is their average length, then the probability distributions of $K_1, K_2, \ldots$ are exponential, i.e.,

$$P(K_i < k) = 1 - e^{-\lambda k}. \tag{1}$$

The parameter λ can be taken as being related to the temperature of the surroundings or the time resolution of the experiment. It follows from Eq. (1) that $U_1, U_2, \ldots$ are transition times for a Poisson process N [23]. At time t, the frequency of the main system (resonance frequency of the central spin or vibrational frequency of the oscillator) can

therefore be written as

$$Q_t = Q_0 + \sum_{i=1}^{N_t} X_i, \tag{2}$$

where Q_0 is an initial frequency and X_i is the frequency change that accompanies the change in the spin environment or new environment oscillator interaction at time U_i. The second assumption is that each X_i is a random variable between $-M$ and $+M$, where M is the bound on the width of the fluctuations that measures the strength of the coupling between the system and environment. The third assumption is that the random variables $X_1, X_2, \ldots$ are independent and are uniformly distributed on the interval $[-M, M]$. For the fluctuating spin model, this means that any spins in environment can flip equal probability. This assumption is valid if the temperature of the environment is high. For the frequency fluctuating oscillator model it means that the range of possible environment molecules that can couple is relatively small. The third assumption is mainly a convenience, because it avoids having to specify the distributions further using more detailed microscopic arguments.

With these assumptions, the process Q is an example of a continuous-time random walk (CTRW) [24], and also a Markov process [25]. Some example trajectories (sample paths) for this CTRW with various values of λ are shown in Fig. 1 (simulated in R 2.12 [26]). Throughout the following, all values of λ are in units of $1/$unit time. This involved simulating an exponential random variable K_1 and keeping the process constant at the value Q_0 for a duration K_1, then simulating a uniform random variable X_1 and another exponential random variable K_2, and keeping the process constant at the value $Q_0 + X_1$ for a duration K_2, and so on.

There are other stochastic models of frequency modulation which assume comparable time scales for the system and surroundings. The Kubo-Anderson process is a prototypic example, in which the frequency takes on one value at a random time, then another random value at another random time, and so on (see, for example, [27]). A more general version of this process, which allows for the Hamiltonian of the oscillator at different times to be noncommutative, was described by Clauser and Blume [19], and was extended further by Dattagupta [28]. Despite appearances, the CTRW in Eq. (2) is actually different. In the Kubo-Anderson process and other former cases the process leaps from one frequency to another in the space of frequencies (state space), irrespective of its current value. Each realization of the process at the jump times is therefore a sequence (not a sum) of independent random variables. On the other hand, at the transition time U_i, the CTRW makes a small frequency change of size X_i. The CTRW therefore undergoes small changes from its current value, rather than completely starting over at each transition time like these other examples do. This is arguably more natural in describing a slowly changing spin environment. It also notes that only a narrow range of environment oscillators could couple to the central oscillator at each transition time, because a frequency close to the frequency of the system would be needed for efficient coupling. Unrestrained leaping across the space of frequencies at each transition time does not necessarily fit this picture. An advantage of working with small changes is that we can express the process as a sum of independent and identically distributed (iid) random variables, as in Eq. (2). This means that the process has a well-defined Gaussian limit, as will be described in the next section. This is not necessarily true for these other processes. For example, one might expect a noise process upon taking the limit of zero waiting times for these other cases, but yet such a process is not a well-defined mathematical object [29]. A well-defined Gaussian limit is preferred for a consistent description of non-Gaussian stochastic dynamics.

A restriction of the CTRW approach is that it is necessarily nonstationary. The distribution and moments of a sum of iid random variables never approach a time-independent state. It is not always clear how to assign random initial conditions to a nonstationary process. Nevertheless we consider a single molecule with a well-defined initial condition, and treat the realizations of its evolution as different repetitions of the experiment. The results we obtain are most suitable for describing dynamics over relatively short, preequilibrium time periods. Nonstationary initial conditions of a process are often useful for describing the dynamics of molecules in an excited environment [30].

A. Moments and distribution of the CTRW process

The moments of Q can be worked out by making use of conditional expectations, namely

$$E\left(Q_t^n\right) = E\left\{E\left[\left(\sum_{i=1}^{N_t} X_i\right)^n \middle| N_t\right]\right\}. \tag{3}$$

Equation (3) says that the nth moment can be worked out by taking N_t as a nonrandom constant, computing the nth moment, and then averaging over N_t. A method for carrying out this calculation is presented in the Appendix and [31]. While no general formula for this step can be given, the second, fourth, and sixth moments work out to be

$$\begin{aligned} E\left(Q_t^2\right) &= \frac{\lambda t M^2}{3}, \\ E\left(Q_t^4\right) &= \frac{\lambda t M^4}{5} + \frac{3\lambda^2 t^2 M^4}{9}, \\ E\left(Q_t^6\right) &= \frac{\lambda t M^6}{7} + \lambda^2 t^2 M^6 + \frac{15\lambda^3 t^3 M^6}{27}, \end{aligned} \tag{4}$$

The odd moments are identically zero. In general, the final term on the right-hand side of each of these equations is of the form $\sigma^n t^{n/2}(n-1)!!$, where $a!! = a(a-2)(a-4)\cdots 1$ is the double factorial and

$$\sigma = \sqrt{\lambda M^2/3}. \tag{5}$$

These terms can therefore be identified with the moments of a Gaussian random variable with mean zero and standard deviation σ. Referring to the other terms in Eq. (4) as the "non-Gaussian contribution," we have the general decomposition

$$E\left(Q_t^n\right) = E_{\text{non-Gaussian}}\left(Q_t^n\right) + \sigma^n t^{n/2}(n-1)!!. \tag{6}$$

The moments of the CTRW process can therefore be thought of as additive corrections to the Gaussian moments.

As $\lambda \to \infty$ and changes in the surrounding environment become more and more rapid compared to the time scale of the

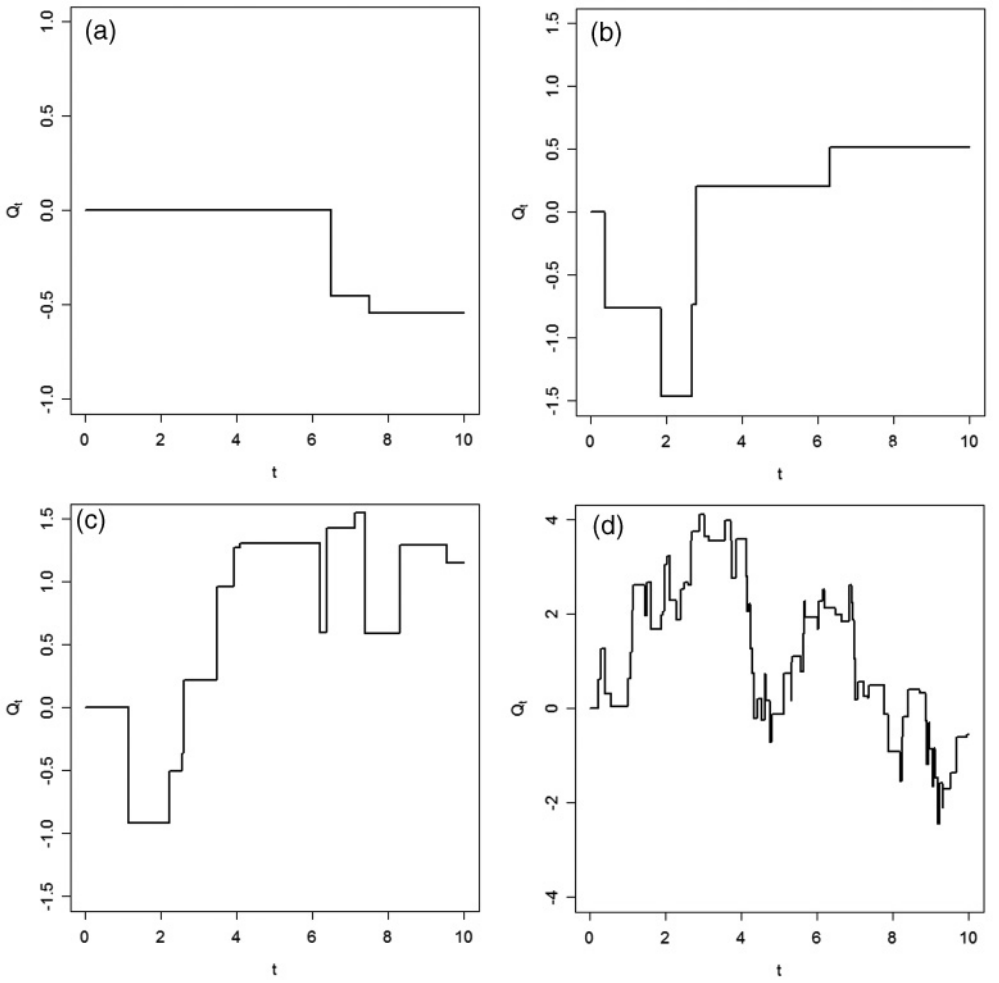

FIG. 1. Representative trajectories of the CTRW process computed with $M = 1$ unit, and (a) $\lambda = 0.1$, (b) $\lambda = 0.5$, (c) $\lambda = 1$, and (d) $\lambda = 10$. A time step of 0.01 was used, and values of λ are in units of 1/unit time (i.e., 1/100 time steps).

system, we might expect that the non-Gaussian contribution to the moments would vanish. However, Eq. (4) shows that both the Gaussian and non-Gaussian terms grow without bound with λ. This occurs because, on its own, the limit $\lambda \to \infty$ does not render the system-environment interactions weak enough for the dynamics to be Gaussian. The size of the frequency modulation due to changes in the state of the environment is given by the parameter M, and so this needs to take on a new value in the limit, i.e., it needs to be renormalized. If we suppose that close to the limit M becomes

$$M = \sqrt{3/\lambda}, \tag{7}$$

then the non-Gaussian term in Eq. (6) vanishes in the limit, and the Gaussian term becomes

$$\sigma^n t^{n/2}(n-1)!! \to t^{n/2}(n-1)!!. \tag{8}$$

The renormalizer in Eq. (7) was chosen so that the limiting Gaussian random variable has the same moments as a Wiener process at time t. This choice is not so arbitrary, because for small λ the Gaussian terms in Eq. (4) are the moments of a Wiener process with time rescaled by a factor of σ.

The renormalized M in Eq. (7) becomes vanishingly small in the Gaussian limit $\lambda \to \infty$. For the spin model, this suggests that at the times $U_1, U_2, \ldots$ only spins that are very far from the central spin may decouple from the system, and new spins can only couple from a large distance away. A possible explanation is that, if a spin that is close to the system becomes particularly unstable, then in the Gaussian limit it is quickly restabilized due to relatively fast spin changes further away from the system, and so does not end up decoupling. For the oscillator model, a very small M means that only environmental oscillators with a frequency very close to the system may couple in the Gaussian limit. This suggests that the coupling between the system and environment oscillators with much different frequencies takes too long to complete, and is interrupted by an oscillator with a much closer frequency before it is finished. Note that a renormalizer of equivalent form was obtained in Ref. [32] in a study of the onset of Ornstein-Uhlenbeck-type dynamics in a simple model of motion in a condensed phase. The reappearance of the renormalizer in Eq. (7) tentatively suggests that it is of more general significance in connecting non-Gaussian and Gaussian-type stochastic dynamics.

The first eight moments of Q_t are plotted in Fig. 2 as a function of λ. M has been set to its limiting value given by Eq. (7) so that we can try and identify a critical value λ_c beyond which the non-Gaussian contribution in Eq. (4) is particularly

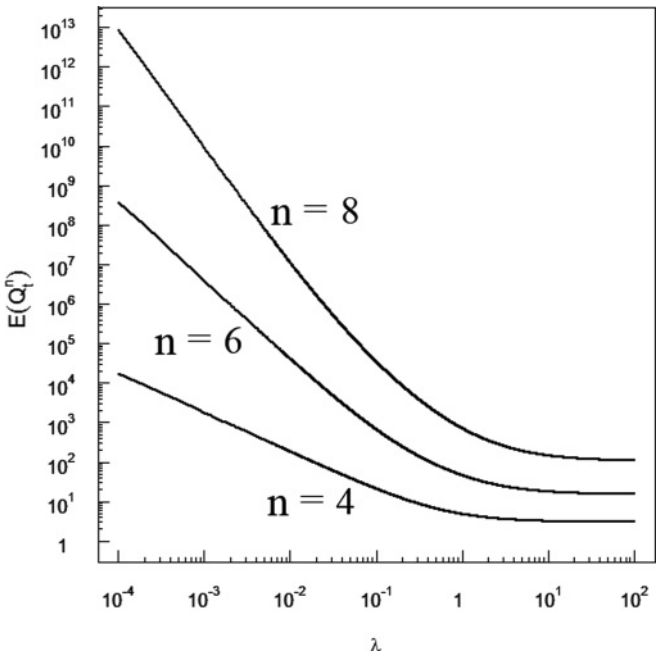

FIG. 2. The fourth, sixth, and eighth moments of Q_t after substituting in the renormalizer Eq. (7). The second moment is constant under renormalization, and so is not plotted.

small. The figure suggests that

$$\lambda_c \approx 10. \tag{9}$$

This value of λ_c looks to be more accurate for the lower moments than the higher moments, because the higher moments appear to converge at successively higher values of λ. We will justify this value of λ_c further at the end of this section.

For later use, we work out the correlation function of the CTRW, using the fact that for $s \leqslant t$, $Q_t - Q_s$ and Q_s are independent random variables. This is because $Q_t - Q_s$ and Q_s are themselves sums of independent random variables Eq. (2), and neither sum contains any common elements. We therefore obtain

$$\begin{aligned} E\left(Q_t Q_s\right) &= E\left\{\left[\left(Q_t - Q_s\right) + Q_s\right] Q_s\right\} \\ &= E\left(Q_s^2\right). \end{aligned} \tag{10}$$

Because the correlation function depends on s explicitly, rather than just on time difference $t - s$, it can be seen that the CTRW process is nonstationary.

The probability density of the CTRW process at time t can be computed in a similar way to the moments. Denote the density by $f(q)$ and let $f(q|N_t = n)$ be the density of Q_t computed as if N_t was fixed at the constant value n. Then we can write

$$\begin{aligned} f(q) &= \sum_{n=0}^{\infty} f(q|N_t = n) P(N_t = n) \\ &= e^{-\lambda t} \sum_{n=0}^{\infty} \frac{\lambda^n t^n}{n!} f(q|N_t = n). \end{aligned} \tag{11}$$

The density $f(q|N_t = n)$ is a density of a sum of n uniform random variables. An expression for this is available (see [33], p. 28), and upon substitution of it into Eq. (11) it yields

$$f(q) = \sum_{n=0}^{\infty} \sum_{k=0}^{n} \frac{e^{-\lambda t} \lambda^n t^n (-1)^k}{(2M)^n n!(n-1)!} \binom{n}{k} [q + (n-2k)M]_+^{n-1}, \tag{12}$$

where $a_+ = a$ if $a > 0$ and is 0 otherwise. Equation (12) is plotted in Fig. 3 for $M = 1$ and $t = 1$ for various values of λ. It was computed by keeping 50 terms in the first sum. Including more terms does not notably affect the distributions in Fig. 3. As λ increases and the environment changes more and more frequently, the distribution of the frequency process broadens from a sharp, leptokurtic spike to a Lorentzian-type curve through to a broad Gaussian-like curve. We will interpret this result further in Sec. III.

Figure 3 allows us to justify the value of λ_c in Eq. (9) further. It is known that the higher moments of a distribution determine the tails of a distribution, and that two distributions whose first several moments are equal have very similar tails [34]. Figure 2 therefore shows that at $\lambda \approx 10$, the tails of the distribution of Q_t are essentially those of a normal distribution. On the other hand, Fig. 3 shows that at small λ the essential difference between the distribution of Q_t and a Gaussian distribution is that the former has much heavier tails (i.e., the tails have larger values and approach zero more rapidly). The similarity of the tails at $\lambda \approx 10$ therefore suggests that at this value the two distributions are quite similar.

The form of Eq. (12) is not so easy to interpret. In fact, using the decomposition (6) we can decompose the density $f(q)$ into a Gaussian density and an additive correction term. The characteristic function of Q_t is

$$\begin{aligned} \phi(k) &= 1 + \sum_{n=1}^{\infty} \frac{i^n k^n E\left(Q_t^n\right)}{n!} \\ &= 1 + \sum_{n=1}^{\infty} \frac{i^n k^n}{n!} \left[E_{\text{non-Gaussian}}\left(Q_t^n\right) + \sigma^n (n-1)!!\right] \\ &= [\phi_{\text{Gaussian}}(k) - 1] + \phi_{\text{non-Gaussian}}(k). \end{aligned} \tag{13}$$

$\phi_{\text{non-Gaussian}}(k)$ is the characteristic function for a random variable with moments given by $E_{\text{non-Gaussian}}(Q_t^n)$. We will assume that such a random variable is well defined. The density function $f(q)$ is found by taking the Fourier transform of Eq. (13), namely

$$\begin{aligned} f(q) &= \left[\int_{-\infty}^{\infty} \phi_{\text{Gaussian}}(k)\, e^{-ikq} dk - \int_{-\infty}^{\infty} e^{-ikq} dk\right] \\ &\quad + \int_{-\infty}^{\infty} \phi_{\text{non-Gaussian}}(k)\, e^{-ikq} dk \\ &= [f_{\text{Gaussian}}(q) - \delta(q)] + f_{\text{non-Gaussian}}(q), \end{aligned} \tag{14}$$

where $\delta(q)$ is a delta function centered on 0 and $f_{\text{Gaussian}}(k)$ is a Gaussian density with standard deviation σ. The second equality in Eq. (13) shows that $\phi_{\text{non-Gaussian}}(k) - 1 \to 0$ as $\lambda \to \infty$ and $E_{\text{non-Gaussian}}(Q_t^n) \to 0$, and so as the moments of the CTRW process converge to those of a Wiener process, the probability density also converges. This is a nontrivial observation, because mathematically, convergence of moments and

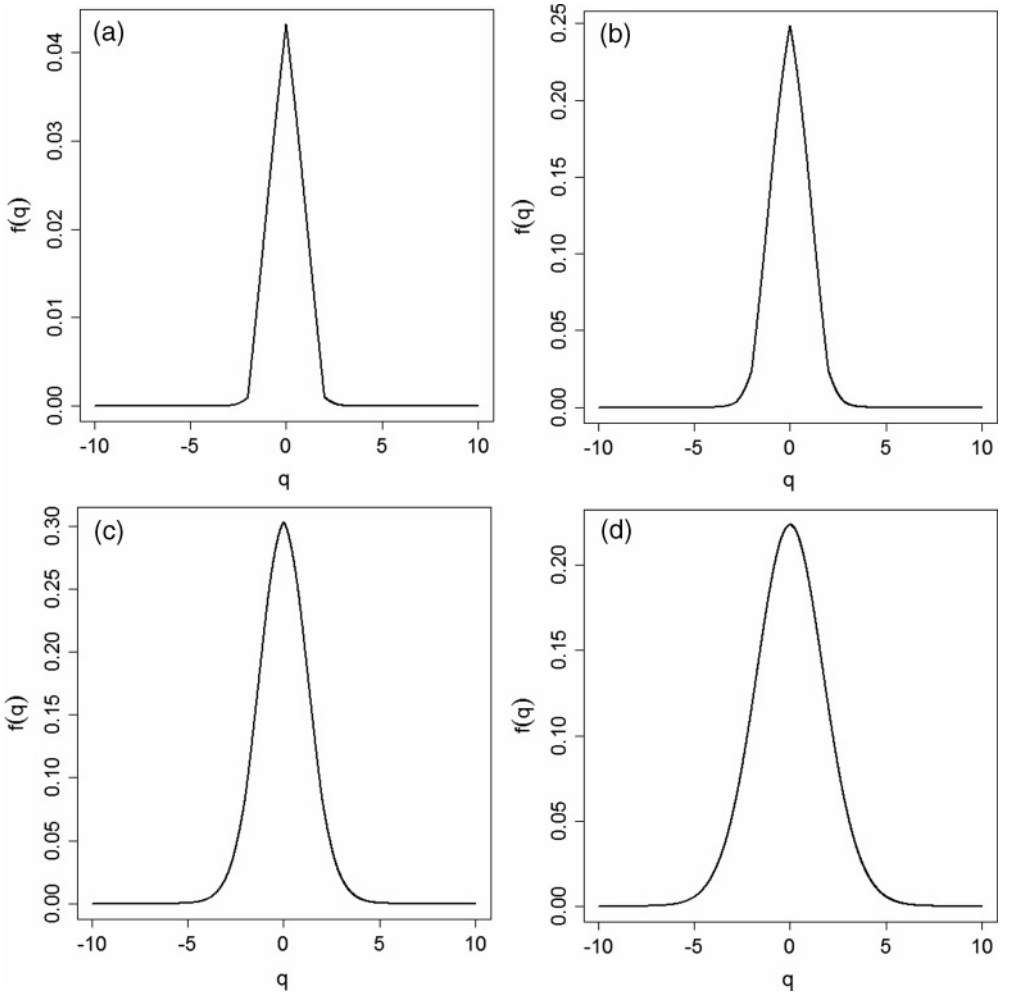

FIG. 3. Plots of the distribution of Q_t [Eq. (12)] computed at $t = 1$ unit, $M = 1$ unit, and (a) $\lambda = 0.5$, (b) $\lambda = 2$, (c) $\lambda = 5$, and (d) $\lambda = 10$.

convergence of probability distributions do not always imply one another [35]. Note that in a strict mathematical sense, the above only proves convergence of the stochastic process at an arbitrary fixed point in time. To prove that the process jointly converges at all fixed times to the Wiener process, we would need to make use of the independence of the increments of the CTRW process, the central limit theorem, and the so-called continuous mapping theorem, and also establish a property called tightness [32,36]. These extra steps do not add to our discussion, so we do not worry about them here.

III. DYNAMICS AND SPECTRAL LINES

A. Spin system

The distribution of the frequency process at time t in Eq. (12) and in Fig. 3 can loosely be interpreted as a magnetic resonance (MR) line of the central spin in the coupled spin model. In fact, it corresponds to the average MR signal of a single spin measured in a single molecule experiment, i.e., the average MR line measured from all possible trajectories of the spin. The breadth of the line represents the fluctuations in the resonance frequency due to interactions with the environment. As can be seen from the moments in Eq. (4), as λ increases and changes in the surrounding environment occur more and more frequently, the distribution becomes broader. Note that for small λ, where the non-Gaussian contributions to the spectrum should be relatively large, the spectrum has a distinctly sharp peak and leptokurtic shape.

In the limit $\lambda \to \infty$, the distribution becomes Gaussian and the standard deviation becomes $\sqrt{t}$. At large but finite λ, the non-Gaussian contribution to the moments in Eq. (4) is relatively small, and so the standard deviation of the distribution is close to $\sigma\sqrt{t}$. Because the renormalizer in Eq. (7) only strictly needs to hold right in the limit, for arbitrary M the distribution at large λ can be broader than the limiting distribution. The MR signal is therefore broader for large λ, non-Gaussian frequency modulation than it is for infinite λ Gaussian modulation. Equation (7) says that individual changes in the surrounding spin environment have a small effect on the resonance frequency of the spin in the Gaussian limit. The resonance frequency therefore changes by a relatively small extent during the MR measurement, and so the line appears more narrow. This observation might correspond to motional narrowing of spectral lines seen in MR experiments, in which as the temperature of the system (here related to λ) increases the line becomes more narrow [22].

B. Oscillator system. Decay of mean displacement

In the case of the spin system given above, the only variable that is available to study is the resonance frequency of the spin and its distribution. However, for the oscillator problem we can investigate the displacement of the oscillator as well as its vibrational spectrum. At time t, the displacement of the oscillator from its equilibrium position is

$$Z_t = z_0 \exp\left(i \int_0^t Q_r dr\right), \tag{15}$$

where the initial condition Q_0 is set to 1. Note that Eq. (15) does not uniquely describe the coordinate of a harmonic oscillator. For example, Z_t could also be interpreted as the angular displacement of a rigid rotor. The non-Gaussian angular frequency Q_t could be understood in terms of random collisions with other rotors after the intervals $K_1, K_2, \ldots$, leading to frequency changes of $X_1, X_2, \ldots$. Throughout the following, we will stick with the oscillator interpretation of Eq. (15).

The dynamics of the oscillator can be broadly described by looking at the mean and variance of Eq. (15). These correspond to averages over the possible trajectories of a single molecule in a single molecule experiment. It does not appear possible to evaluate the expectation of the right-hand side of Eq. (15) without approximating the integral. By the mean value theorem, the integral can be written as

$$\int_0^t Q_r dr = Q_h t, \tag{16}$$

where h is a time in $(0,t)$ that depends on t. When λ is very small and t does not greatly exceed $1/\lambda$, then with high probability the sample paths of Q will not fluctuate too wildly in the interval $(0,t)$. The time average of most trajectories of Q over the interval $(0,t)$ will not therefore change so greatly with t, and so we can approximate Eq. (16) with

$$\int_0^t Q_r dr \approx Q_t t. \tag{17}$$

The expected value of Z_t under this approximation is worked out in the Appendix. It is

$$E(Z_t) = e^{-\lambda t} \exp\left[\frac{\lambda}{M} \sin(Mt)\right]. \tag{18}$$

Figures 4(b)–4(d) illustrate Eq. (18) for $M = 1$ and various small λ. The curves are compared to averages estimated from

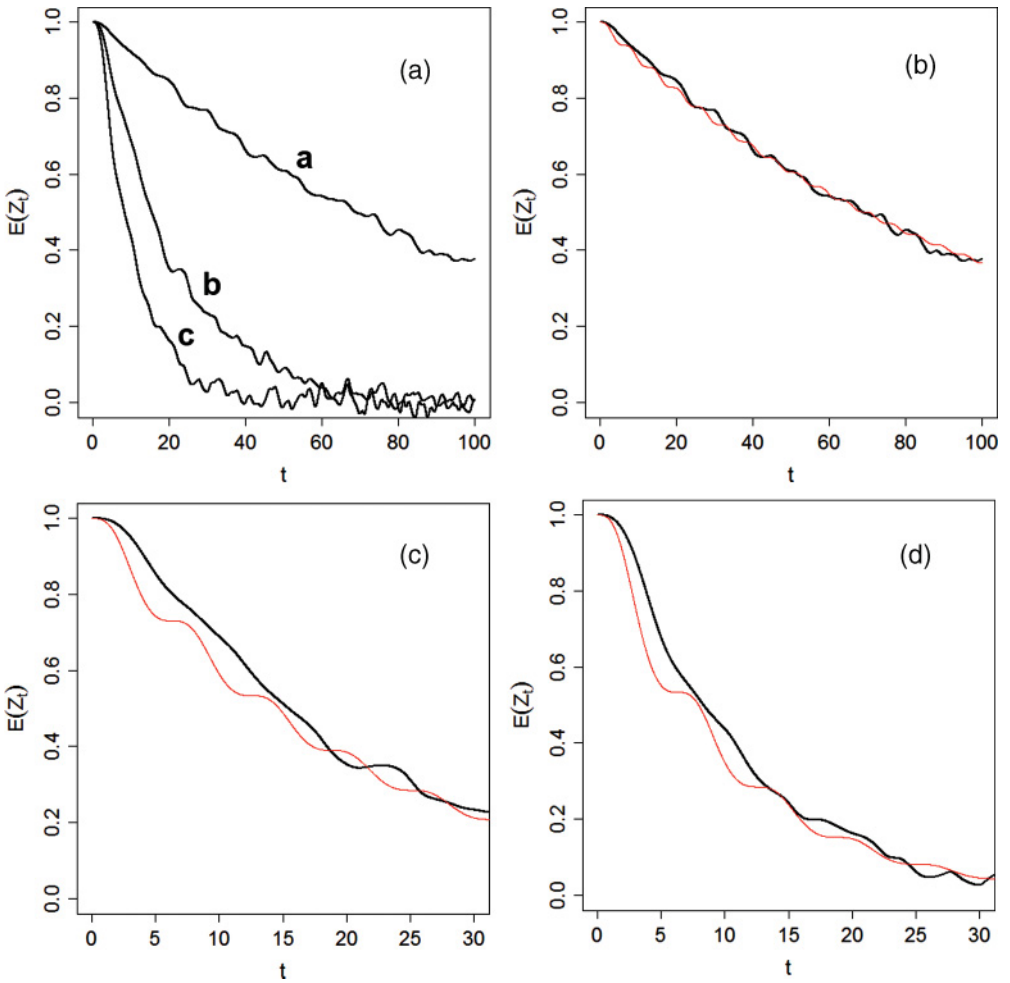

FIG. 4. (Color online) Plots of $E(Z_t)$ for small λ estimated from numerical simulations, using $M = 1$ unit and a time step of 0.01. Plot (a) compares the cases a $\lambda = 0.01$, b $\lambda = 0.05$, and c $\lambda = 0.1$. The analytic formula Eq. (18) (thin red curve) is compared to the numerical results (thick black curve) for (b) $\lambda = 0.01$, (c) $\lambda = 0.05$, and (d) $\lambda = 0.1$.

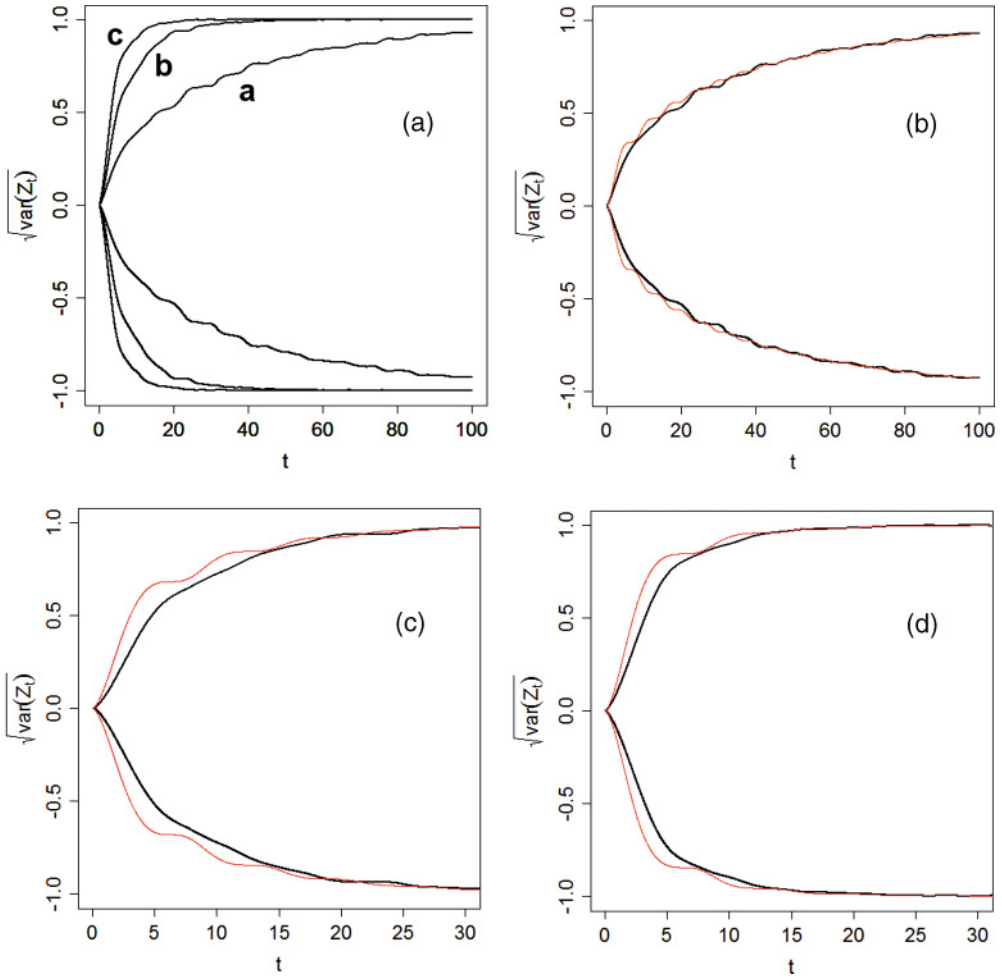

FIG. 5. (Color online) Plots of the rms displacement $\pm\sqrt{\text{var}(Z_t)}$ for each of the cases in Fig. 4.

2000 simulations of the oscillator displacement process, as computed in R 2.12.0 using the method to simulate trajectories of the frequency fluctuation process described at the end of Sec. II A and the trapezium rule to handle the integral. The simulated curves are compared directly in Fig. 4(a). It can be seen that the simulated curves do not decay smoothly to their equilibrium value. These features are most obvious for the $\lambda = 0.01$ curve, which decays via a series of small steps. Averaging over further trajectories does not eliminate the presence of these features. Equation (18) agrees with the simulated $\lambda = 0.01$ curve reasonably well, predicting the correct height of the steps in the decay curve and in some cases getting the steps in the correct place. These steps can be understood in terms of "beating" between different trajectories in the ensemble of possible trajectories for the diatomic molecule. Thus, at small λ and after short times the vibrational frequencies of the oscillators in the ensemble will only differ from one another by a small amount, causing the oscillation phases across the ensemble to match periodically. The smaller the value of λ, the less the variation in oscillation frequencies across the ensemble, and so the shorter this period becomes. Equation (18) does not compare as well to the simulated curves for the cases $\lambda = 0.05$ and $\lambda = 0.1$, but nonetheless suggests that the bumpy decay of these curves can also be traced to beating across the ensemble.

The variance of the oscillator displacement is

$$\begin{aligned}\text{var}(Z_t) &= E(Z_t Z_t^*) - E(Z_t)^2 \\ &= 1 - E(Z_t)^2. \end{aligned} \tag{19}$$

The first equality is permitted so long as we are only interested in the real part of Z_t. Substituting Eq. (18) into Eq. (19) gives, for small λ,

$$\text{var}(Z_t) = 1 - e^{-2\lambda t}\exp\left[\frac{2\lambda}{M}\sin(Mt)\right]. \tag{20}$$

The root mean square (rms) displacement of the oscillator, $\pm\sqrt{\text{var}(Z_t)}$, is plotted in Fig. 5 for each of the cases in Fig. 4 and again compared to numerical estimates. Beating is again for the $\lambda = 0.01$ case, this time as a series of plateaus that the rms displacement goes through as it increases spreads from its initial zero value. Weaker irregular features are also seen for $\lambda = 0.05$ and $\lambda = 0.1$ cases.

With larger values of λ [larger than about ten interactions per unit time, according to Eq. (9)], the frequency variation across the ensemble would be very large, even for relatively short times. The oscillation phases across the ensemble would almost never match, and so we would expect for $E(Z_t)$ to decay in a relatively smooth manner. When λ is very large, the non-Gaussian terms in Eqs. (4)

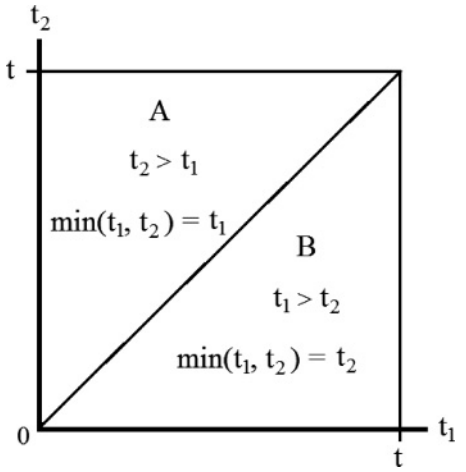

FIG. 6. Diagram showing integration domain for Eq. (21). The diagonal line is $t_2 = t_1$.

and (14) are negligible and Q_t is approximately a Gaussian random variable [with standard deviation given by Eq. (5)]. M does not necessarily take on its renormalized value in Eq. (7), because that only needs to hold very close to the limit $\lambda \to \infty$, and not necessarily for arbitrarily large λ. $E(Z_t)$ can be computed approximately using the Gaussian result

$$E(Z_t) \approx \exp\left[-\frac{1}{2}\int_0^t\int_0^t E\left(Q_{t_1}Q_{t_2}\right)dt_1dt_2\right] = \exp\left[-\frac{1}{2}\int_0^t\int_0^t E\left(Q^2_{\min(t_1,t_2)}\right)dt_1dt_2\right], \quad (21)$$

where we have substituted in Eq. (10). The integral in Eq. (21) is over the square area $(0,t)\times(0,t)$, which can be divided into two triangular areas A and B. In region A $\min(t_1,t_2) = t_1$, whereas in region B $\min(t_1,t_2) = t_2$ (Fig. 6). We can therefore write

$$\begin{aligned}&\int_0^t\int_0^t E\left(Q_{t_1}Q_{t_2}\right)dt_1dt_2\\ &= \frac{1}{2}\int\int_A E\left(Q_{t_1}Q_{t_2}\right)dt_1dt_2 + \frac{1}{2}\int\int_B E\left(Q_{t_1}Q_{t_2}\right)dt_1dt_2\\ &= \frac{1}{2}\int_0^t dt_2\int_0^{t_2} dt_1 E\left(Q^2_{t_1}\right) + \frac{1}{2}\int_0^t dt_1\int_0^{t_1} dt_2 E\left(Q^2_{t_2}\right),\end{aligned} \quad (22)$$

and so, using Eq. (4),

$$E(Z_t) \approx \exp\left(-\frac{\lambda M^2 t^3}{18}\right). \quad (23)$$

Figure 7(a) illustrates Eq. (23) using $M = 1$ and various λ, and is compared to numerical calculations. For these cases, the curve is indeed a smooth monotonic decay, and there is no occurrence of beating among different trajectories in the ensemble. Using Eq. (19), the variance works out to be

$$\mathrm{var}(Z_t) = 1 - \exp\left(-\frac{\lambda M^2 t^3}{9}\right). \quad (24)$$

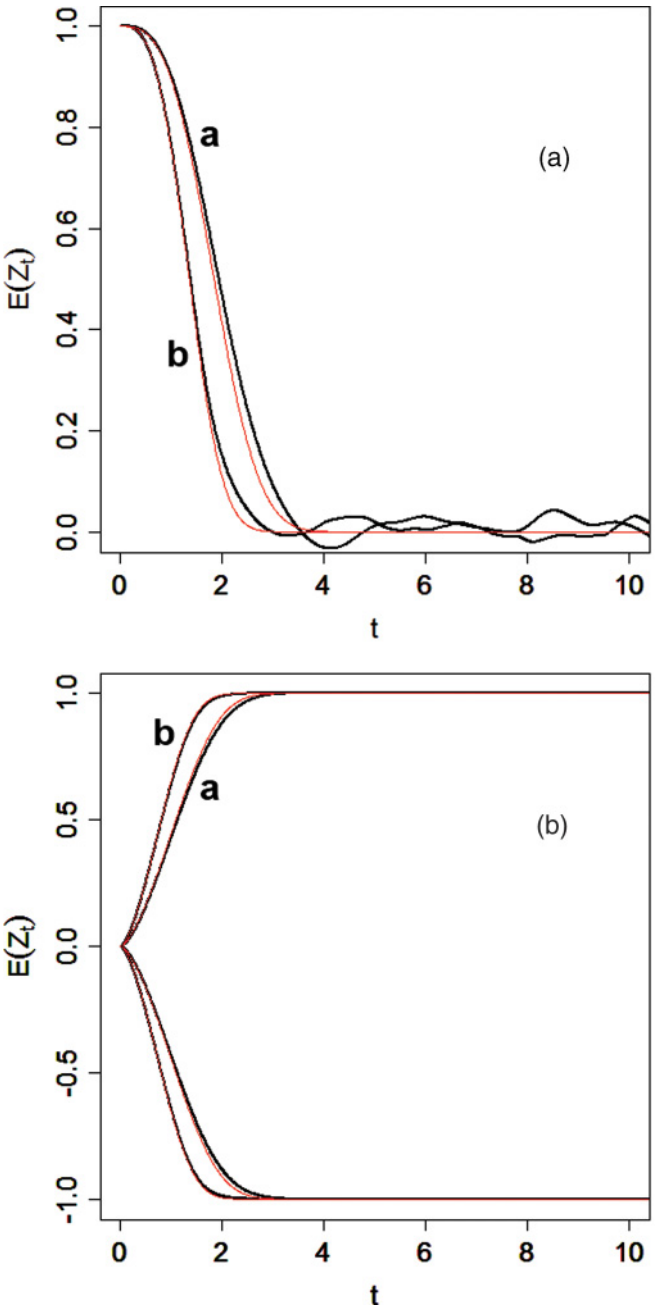

FIG. 7. (Color online) Plots of (a) $E(Z_t)$ and (b) the rms displacement for large λ estimated by numerical simulations (thick black lines) using $M = 1$ and a time step of 0.01, and compared to the analytic formula Eq. (18) (thin red lines) for the cases a $\lambda = 2$ and b $\lambda = 5$.

The rms displacement for the high λ case is plotted in Fig. 7(b), and is seen to spread in a smooth manner from zero. The results obtained here suggest that beating of the average trajectory of a molecule is a signature of slow, non-Gaussian frequency modulation. It would be interesting to investigate it in the laboratory, possibly using Eq. (18) to help estimate a value of λ.

In the limit $\lambda \to \infty$, the frequency fluctuation process Q converges to a Wiener process and M takes on the renormalized value in Eq. (7). Proceeding as we did to work out Eq. (23), but using $E(W_{t_1}W_{t_2}) = E(W^2_{\min(t_1,t_2)}) = \min(t_1,t_2)$ in place of

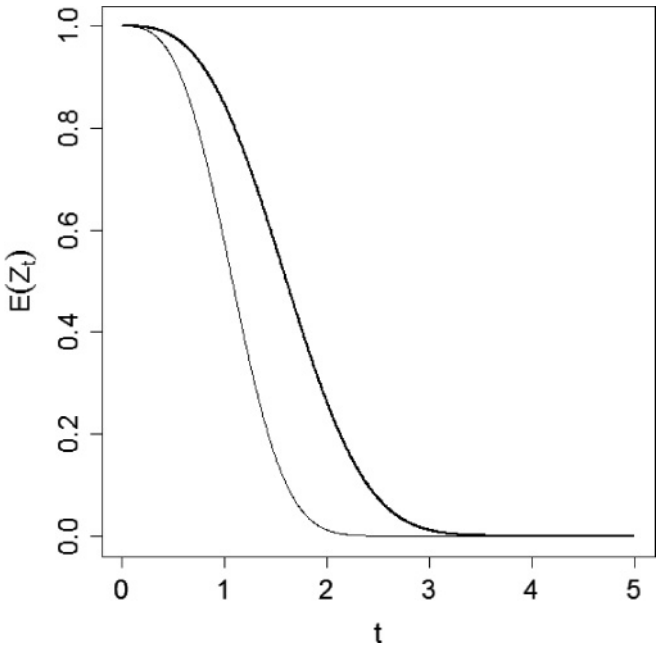

FIG. 8. Plots of Eq. (23) for $M = 1$ and $\lambda = 10$ (thin line) and Eq. (25) (thick line). Equation (25) corresponds to the limit $\lambda \to \infty$, $M \to \sqrt{3/\lambda}$.

$E(Q_{t_1} Q_{t_2})$ in Eq. (21), we obtain

$$E(Z_t) = e^{-t^3/6}. \tag{25}$$

Equations (23) and (25) are compared in Fig. 8, using $M = 1$ and $\lambda = 10$, which lies near the transition point Eq. (9). It is seen that the high lambda average described by Eq. (23) relaxes to its equilibrium state more quickly than the infinite lambda, Gaussian case described by Eq. (25), despite the observation in Figs. 4(a) and 7(a) that $E(Z_t)$ decays more rapidly for larger λ. In Sec. II A, the renormalized M was interpreted to mean that only environmental oscillators with a frequency very close to the system may couple in the limit. Here we see that relaxation of a oscillator from its initial displacement by rapid successive interactions with the environment is inefficient when the interactions are restricted in this way. Similar comments apply to the rms displacement in the limiting case (result not shown here).

C. Oscillator system. Vibrational spectra

Similar to what we had with the discussion of line shapes in the spin problem, the spectra discussed here correspond to the average spectrum measured from a single molecule trajectory. Such a spectrum is the Fourier transform of the correlation function of its dipole moment, where the correlation function is taken over all possible trajectories of the molecule. In turn, the dipole moment is proportional to the oscillator displacement Z_t, and so we can write the spectrum of the oscillator as

$$I(q) = \frac{1}{2\pi} \int_{-\infty}^{+\infty} E\,(Z_t Z_{t+s}) e^{-iqs} ds. \tag{26}$$

Equation (26) is a version of the Wiener-Khinchin theorem, and only holds when $E(Z_t Z_{t+s})$ is independent of t and only depends upon the time difference s (i.e., when Z is a stationary process) [1]. Because Q is not a stationary process, we cannot expect that Z is stationary. However, there is a theorem which says that the Wiener-Khinchin theorem holds for a nonstationary process if $E(Z_t Z_{t+s})$ is replaced by $\langle E(Z_t Z_{t+s})\rangle$, its long time-averaged value [mean value in t over a wide time interval $[-T, T]$ [37]. The following will therefore employ time-averaged correlation functions.

We first show that for small λ the spectrum can be decomposed into Gaussian and non-Gaussian components. Using the formula $E(Z_{t+s} Z_t) = E(Z_{t+s} Z_t^*)$ and the approximation discussed in the previous section, we have

$$E(Z_{t+s} Z_t) \simeq E(e^{isQ_s}). \tag{27}$$

The choice of time s in the exponent is allowed because we are assuming that the trajectories of the CTRW process do not vary too much over all times of interest. Equation (27) is the characteristic function of Q_s evaluated at s. It can be decomposed into a Gaussian and non-Gaussian component as in Eq. (13), and so, after time averaging and integrating, Eq. (26) takes on the form

$$I(q) = [I_{\text{Gaussian}}(q) - \delta(q)] + I_{\text{non-Gaussian}}(q). \tag{28}$$

In the small λ regime where Eq. (28) applies, the term $I_{\text{Gaussian}}(q) - \delta(q)$ makes a relatively small contribution. Figure 9 plots the spectra estimated from 1000 to 2000 simulations of the displacement process Z_t for $\lambda = 0.1$ and 0.5. This was done by estimating the autocorrelation function $E(Z_{t+s} Z_t)$ for each sample using R 2.12.0 (via the acf subroutine, which averages over all t), fast Fourier transforming the result (via the spec.ar subroutine, which smoothes the spectrum by fitting an autoregressive model to

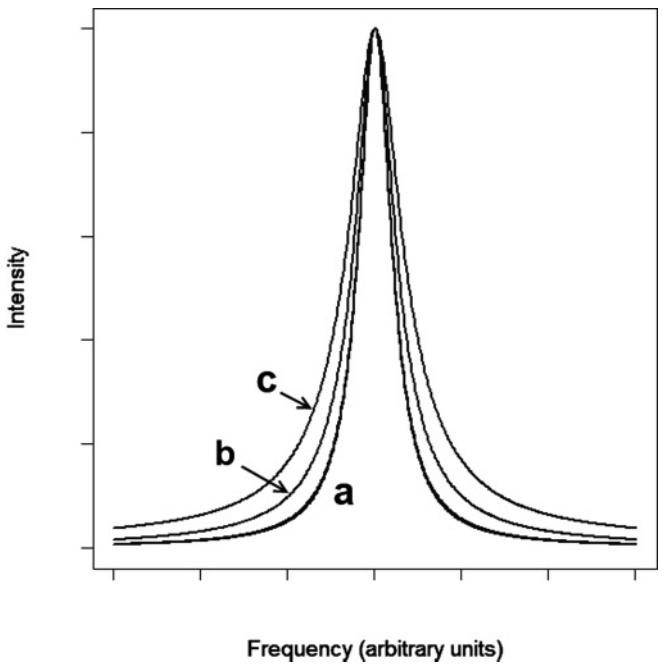

FIG. 9. Spectra estimated from trajectory simulations using $M = 1$, a time step of 0.01, and a $\lambda = 0.1$ and $\lambda = 0.5$ (overlapping curves), b $\lambda = 2$, and c $\lambda = 5$. See text for calculation details. The spectra are centred on zero frequency and the intensity axis goes from 0 to 1. Each spectrum is normalised to have unit intensity at its maximum.

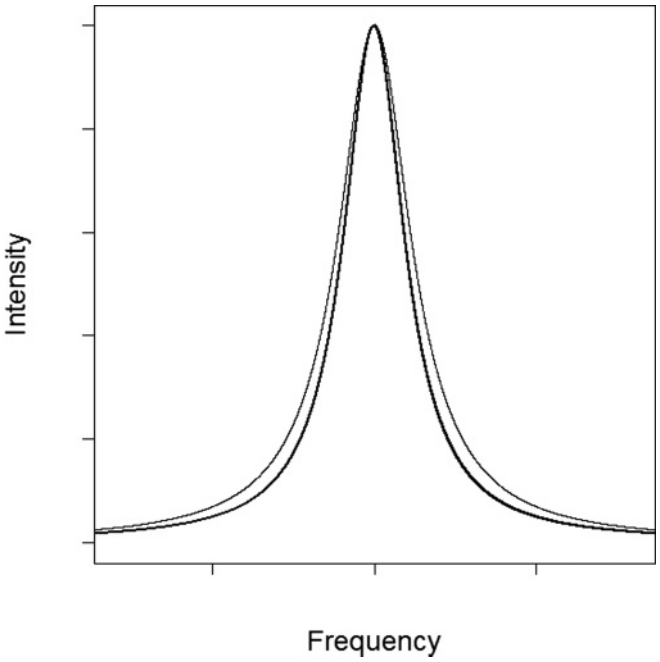

FIG. 10. Spectra estimated by fast Fourier transforms of Eq. (34) with $M = 1$ and $\lambda = 10$ (thin line) and of Eq. (35) (thick line). Equation (35) corresponds to the limit $\lambda \to \infty$, $M \to \sqrt{3/\lambda}$. The spectra are centred on zero frequency and the intensity axis goes from 0 to 1. Each spectrum is normalised to have unit intensity at its maximum.

it) and averaging over the spectra. The two curves overlap, and there is essentially no difference between them. At these values of λ we can suppose that only the non-Gaussian term in Eq. (28) makes any significant contribution, and so that the spectra for $\lambda = 0.1$ and 0.5 in Fig. 10 essentially represent $I_{\text{non-Gaussian}}(q)$. Figure 9 therefore shows that the non-Gaussian component takes the form of a narrow, Lorentzian-type curve, which slowly broadens as λ increases. In fact, in the limit $\lambda \to 0$ we have $Q_t = Q_0 = 0$ with probability 1 and

$$E(Z_t Z_{t+s}) = E\left[\exp\left(i\int_t^{t+s} Q_r dr\right)\right] \to 1. \tag{29}$$

Substituting Eq. (29) into Eq. (27) gives

$$\lim_{\lambda\to\infty} I(q) = \delta(q), \tag{30}$$

and so for extremely small λ, $I(q) \approx I_{\text{non-Gaussian}}(q) \approx \delta(q)$. The narrowness of these lines at small λ reflects the fact that, when the occurrence of new oscillator-environment interactions is relatively rare, the oscillator can only explore a relatively limited range of frequencies over a typical measurement period.

Figure 9 also shows spectra estimated for the cases $\lambda = 2$ and $\lambda = 5$, where the Gaussian character of the spectrum should be more discernable. Like the non-Gaussian spectra, these higher λ spectra also take the form of a narrow Lorentzian-type curve, broadening slightly as λ increases. The similarity of shape between the two types of spectra suggests that the Gaussian and non-Gaussian stochastic dynamics cannot be distinguished by the shapes of linear spectra alone.

The high λ case can be computed approximately without trajectory simulations. When λ is large enough for Q_t to be approximately a Gaussian random variable, but not so large that M needs to be renormalized, we can write

$$\begin{aligned} E(Z_{t+s}Z_t) &\approx \exp\left[-\frac{1}{2}\int_t^{t+s}\int_t^{t+s} E\left(Q_{t_1}Q_{t_2}\right)dt_1dt_2\right] \\ &= \exp\left[-\frac{1}{2}\int_t^{t+s}\int_t^{t+s} E\left(Q^2_{\min(t_1,t_2)}\right)dt_1dt_2\right], \end{aligned} \tag{31}$$

where we have used the formula $E(Z_{t+s}Z_t) = E(Z_{t+s}Z_t^*)$ to obtain the first equality and Eq. (10) for the second. Proceeding as in Eqs. (23) and (31) works out to be

$$\langle E\left(Z_{t+s}Z_t\right)\rangle \approx \exp\left(-\frac{\lambda M^2 s^3}{36}\right)\left\langle\exp\left(-\frac{\lambda M^2\,|t|\,s^2}{12}\right)\right\rangle. \tag{32}$$

The angular brackets indicate an averaging with respect to t over a large time interval. t has been replaced with its absolute value so that the averaging can be carried over to negative times. The term in the angular brackets is twice the average value of an exponential decay over a long period of time, which is a very small quantity that does not appreciably change with ordinary values of s. It can therefore be regarded as a constant, and Eq. (32) can be rewritten as

$$\langle E\left(Z_{t+s}Z_t\right)\rangle \propto \exp\left(-\frac{\lambda M^2 s^3}{36}\right). \tag{33}$$

For the case where $\lambda \to \infty$ and the CTRW process converges to a Wiener process, we obtain

$$\begin{aligned} \langle E(Z_{t+s}Z_t)\rangle &= e^{-s^3/6}\langle e^{-|t|s^2/2}\rangle \\ &\propto e^{-s^3/6}. \end{aligned} \tag{34}$$

Fast Fourier transform of Eqs. (34) and (33) gives the spectra shown in Fig. 10. They were computed with $\lambda = 10$ and $M = 1$. The limiting curves still have a Lorentzian appearance; however, the Gaussian case where $\lambda \to \infty$ is slightly more narrow than the high λ case. Similar to the spin system, this line narrowing is due to the weakness of the individual oscillator-environment oscillator interactions in the limit. The restriction to interactions with environment oscillators with a frequency very close to the system means that the oscillator explores a relatively restricted range of frequencies in the Gaussian limit. Again, this result may correspond to motional narrowing that is seen in experimental IR spectra [22].

IV. FINAL REMARKS

Throughout this paper, we have taken "non-Gaussian dynamics" to mean that the time scale of the system's motion is comparable to the time scale of the motion of the surrounding degrees of freedom. This interpretation is not unique; however, it provides an obvious situation where approximations based on the central limit theorem should not work. We used this concept to construct a simple non-Gaussian stochastic process describing the motion of the environment. This process assumed that the system stayed interacting with one particular state of the environment up to a random length of time, then with another particular state of the environment up to another length of time, and so forth. This is a special case

of a continuous-time random walk. To a large extent, the statistical properties of this process were shown to decompose into Gaussian and non-Gaussian contributions, with the former playing the dominant role when the frequency of new environment states was more than about ten per unit time. It is therefore reasonable to regard our non-Gaussian, continuous-time random walk process in terms of additive corrections to a Gaussian process. This concept was useful at several points in this work, and future investigations could look at whether it allows for approximations based on established results for Gaussian processes; for example, whether product moments such as $E(Q_{t_1}Q_{t_2}\cdots Q_{t_n})$ can be approximately decomposed into sums of products of two-time correlation functions.

To investigate the physical dynamics that come about from this process, we looked at a spin and an oscillator system whose frequencies are modulated as described above. More attention was given to the oscillator system, because that provides an extra variable that can be studied—the displacement as a function of time—in addition to its frequency. The oscillator displacement, when averaged over all possible trajectories from a given initial point, showed beating between different trajectories in the average when the occurrence of new interactions was extremely infrequent. This feature vanished when the Gaussian contributions to the process became more important, and so it might be regarded as a signature of non-Gaussian dynamics for the oscillator system. If this situation could be replicated in the laboratory, then it might allow for measurement of the average frequency at which the surrounding environment changes (i.e., of the parameter λ in the main text). Throughout the paper, it was emphasized that changes in the state of the surrounding environment can only have a very small influence on the system's evolution in order for the Gaussian limit to be meaningful. As a consequence of this, we saw that the (trajectory-averaged) resonance spectrum of the spin system and vibrational spectrum of the oscillator were more narrow when the frequency at which the surroundings changed was infinite than when it was a large, but finite, value of the frequency. If we take larger values of λ to mean a larger temperature of the environment, then this narrowing probably corresponds with motional narrowing seen in experimental spectra [22].

Because the non-Gaussian concepts were developed by explicitly considering the spin and oscillator problems, our approach might appear very application dependent and difficult to apply in more general settings. A more general framework might be provided by the stochastic Liouville equation, which in the quantum case reads as

$$\frac{d\hat{\rho}}{dt} = -\frac{i}{\hbar}[\hat{H}_0 + \hat{V}_Q, \hat{\rho}], \tag{35}$$

where $\hat{\rho}$ is the density operator of the system, $\hat{H}_0$ the system Hamiltonian, and $\hat{V}_Q$ an operator which couples the CTRW stochastic process Q to the system [38]. The stochastic Liouville equation in the above form is a particularly useful starting point for spectroscopic problems. Applying it would involve integrating it for a sample of trajectories of the CTRW process, and then estimating the relevant statistics. Note that the integration step would require certain specialized mathematical techniques to handle the discontinuities of the trajectories of the CTRW process, as well as to ensure that the solutions remain stable as we approach the Gaussian limit [39]. Like our own treatment of the spin and oscillator problems, Eq. (35) does not account for energy dissipation from the system to the surroundings. This is no significant difficulty when dynamics over relatively short time scales are of interest, but it is a problem over longer time scales where equilibrium distributions become important. More sophisticated versions of the stochastic Langevin equation are available, in which dissipation is incorporated by means of path integral techniques [40,41]. Stochastic differential equations and the Langevin equation also provide a means to tackle mechanical problems with and without dissipation [42]. The CTRW process could appear in these as the random force term, and would be best implemented by means of the "Ito" representation dQ_t/dt. This would involve changes via a series of randomly spaced spikes, each representing the occurrence of a new system-environment interaction.

As well as the above, future studies might try and apply the above to problems in nonlinear response theory. This would allow the above ideas to be tested against data collected from nonlinear spectroscopy experiments, in which several instances of non-Gaussian dynamics have been observed.

ACKNOWLEDGMENT

D. M. P. is supported by the Japan Society for the Promotion of Science.

APPENDIX

1. Formula for the moments of a sum of iid random variables

Let $X_1, X_2, \ldots$ be a sequence of iid random variables that have the same distribution as a random variable X, and N_t the value of a Poisson process at time t. We assume that the random variable N_t is independent of X. The pth moment of the sum

$$Q_t = \sum_{i=1}^{N_t} X_i \tag{A1}$$

can be worked out as follows. Define a collection of products of moments of X:

$$C = \left\{ E(X^r)E(X^s)\cdots E(X^u) : \begin{matrix} r,s,\ldots,u \in \{1,2,\ldots,p\} \\ r+s+\cdots+u = p \end{matrix} \right\}. \tag{A2}$$

The pth moment of Q_t is

$$\begin{aligned} E\left(Q_t^p\right) &= E\left[E\left(Q_t^p \middle| N_t\right)\right] \\ &= \sum_{q_i \in C} E(A_i) q_i, \end{aligned} \tag{A3}$$

where, for $q_i = E(X^{p_1})E(X^{p_2})\cdots E(X^{p_m})$,

$$\begin{aligned} E(A_i) &= \frac{1}{l_1!l_2!\cdots l_h!} E\left[\frac{N_t!}{(N_t-m)!}\right] \frac{p!}{p_1!p_2!\cdots p_m!} \\ &= \frac{\lambda^m t^m}{l_1!l_2!\cdots l_h!} \frac{p!}{p_1!p_2!\cdots p_m!}. \end{aligned} \tag{A4}$$

In Eq. (A4), h is the number of distinct constants in the sequence $\{p_1, p_2, \ldots, p_m\}$, l_1 the number equal to the first constant, l_2 the number equal to the second constant, ..., and

l_h the number equal to the hth constant. Further explanation and proof of Eqs. (A3) and (A4) can be found in Ref. [31]. The second formula in Eq. (A4) was obtained with a formula of Noras for the moments of a Poisson random variable [43].

2. Derivation of Eq. (18)

Equation (17) of the main text requires evaluation of

$$E(Z_t) \approx E(e^{itQ_t}), \tag{A5}$$

which is the characteristic function of the random variable $tQ_t = \sum_{i=1}^{N_t} tX_i$. This can be done via the conditioning argument

$$\begin{aligned} E\left(e^{i\sum_{j=1}^{N_t} tX_j}\right) &= E\left[E\left(e^{i\sum_{j=1}^{N_t} tX_j}\middle| N_t\right)\right] \\ &= E\left(\phi_{xt}^{N_t}\right), \end{aligned} \tag{A6}$$

where $\phi_{xt} = E(e^{iXt})$. The second quantity follows from the fact that $X_1, X_2, \ldots$ are iid random variables with the same distribution as X. ϕ_{xt} is a nonrandom quantity, and so the only random variable that $\phi_{xt}^{N_t}$ depends upon is N_t. The second expectation in Eq. (A8) can therefore be evaluated with respect to the Poisson distribution. This gives

$$\begin{aligned} E\left(\phi_{xt}^{N_t}\right) &= \sum_{n=0}^{\infty} \phi_{xt}^n e^{-\lambda t}(\lambda t)^n/n! \\ &= e^{-\lambda t} e^{\lambda t \phi_{xt}}. \end{aligned} \tag{A7}$$

Similarly, the only random quantity in e^{iXt} is X. ϕ_{xt} can therefore be evaluated by averaging with respect to the uniform distribution over $[-M, M]$, which yields

$$\begin{aligned} E(e^{iXt}) &= \int_{-M}^{M} e^{ixt} \frac{1}{2M} dx \\ &= \frac{1}{Mt} \sin Mt. \end{aligned} \tag{A8}$$

Substituting Eq. (A8) into Eq. (A7) gives Eq. (18) of the main text.

[1] C. W. Gardiner, *Handbook of Stochastic Methods for Physics, Chemistry and the Natural Sciences*, 3rd ed. (Springer, Berlin, 2004).
[2] N. G. van Kampen, *Stochastic Processes in Chemistry and Physics*, 3rd ed. (North-Holland, Amsterdam, 2007).
[3] T. Steinel, J. B. Asbury, S. A. Corcelli, C. P. Lawrence, J. L. Skinner, and M. D. Fayer, Chem. Phys. Lett. **386**, 295 (2004).
[4] T. I. C. Jansen, D. Cringus, and M. S. Pshenichnikov, J. Phys. Chem. A **113**, 6260 (2009).
[5] S. Roy, M. S. Pshenichnikov, and T. L. C. Jansen, J. Phys. Chem. B **115**, 5431 (2011).
[6] A. Baura, M. Kumar Sen, G. Goswami, and B. Chandra Bag, J. Chem. Phys. **134**, 44126 (2011).
[7] E. Milotti, Phys. Rev. E **83**, 42103 (2011).
[8] S. V. Melkonyan, Physica B **405**, 379 (2010).
[9] G. Augello, D. Valenti, and B. Spagnolo, Eur. Phys. J. B **78**, 225 (2010).
[10] J. Danon and P. W. Brouwer, Phys. Rev. Lett. **105**, 136803 (2010).
[11] H. K. Shin, C. Kim, P. Talkner, and E. K. Lee, Chem. Phys. **375**, 316 (2010).
[12] A. d'Onofrio and A. Gandolfi, Phys. Rev. E **82**, 61901 (2010).
[13] J. L. Skinner and W. E. Moerner, J. Phys. Chem. **100**, 13251 (1996).
[14] Y. Tanimura, H. Takano, and J. Klafter, J. Phys. Chem. **108**, 1851 (1998).
[15] J. N. Onuchic and P. G. Wolynes, J. Chem. Phys. **98**, 2218 (1993).
[16] Y. Tanimura, V. B. P. Leite, and J. N. Onuchic, J. Chem. Phys. **117**, 2172 (2002).
[17] Y. Suzuki and Y. Tanimura, J. Chem. Phys. **126**, 54504 (2007).
[18] Y. Tanimura and A. Ishizaki, Acc. Chem. Res. **42**, 1270 (2009).
[19] M. J. Clauser and M. Blume, Phys. Rev. B **3**, 583 (1971).
[20] S. Duttagupta, *Relaxation Phenomena in Condensed Matter Physics* (Academic Press, Orlando, FL, 1987).
[21] R. Durrett, *Probability—Theory and Examples*, 4th ed. (Cambridge University Press, New York, 2010).
[22] R. Kubo, Adv. Chem. Phys. **15**, 101 (1969).
[23] I. Miller and M. Miller, *John E. Freund's Mathematical Statistics with Applications*, 7th ed. (Pearson Prentice-Hall, Upper Saddle River, NJ, 2004).
[24] R. Metzler and J. Klafter, Phys. Rep. **339**, 1 (2000).
[25] P. G. Hoel, S. C. Port, and C. J. Stone, *Introduction to Stochastic Processes* (Houghton Mifflin Company, Boston, 1972).
[26] R Development Core Team, R: A Language and Environment for Statistical Computing (R Foundation for Statistical Computing, Vienna, Austria, 2010), http://www.R-project.org/.
[27] M. Olszewski and N. A. Sergeev, Z. Naturforsch. **63a**, 688 (2008).
[28] S. Dattagupta, Phys. Rev. B **16**, 158 (1977).
[29] B. Oksendal, *Stochastic Differential Equations—An Introduction with Applications*, 6th ed. (Springer-Verlag, Berlin, 2003).
[30] S. Kawai and T. Komatsuzaki, J. Chem. Phys. **134**, 114523 (2011).
[31] D. M. Packwood, e-print arXiv:1105.6283v1 [math.ST] (2011).
[32] D. M. Packwood, J. Phys. A: Math. Theor. **43**, 465001 (2010).
[33] W. Feller, *An Introduction to Probability and Its Applications*, 2nd ed., Vol. II (John Wiley and Sons, New York, 1971).
[34] B. G. Lindsay and P. Basak, Am. Stat. **54**, 1 (2000).
[35] A. W. van der Vaart, *Asymptotic Statistics* (Cambridge University Press, Cambridge, UK, 1998).
[36] R. Durrett, *Stochastic Calculus—A Practical Introduction* (CRC Press, Boca Raton, FL, 1996).
[37] W. Lu and N. Vaswani, e-print arXiv:0904.0602v1 [math.ST] (2009).
[38] P. Hakansson and P. B. Nair, PhysChemChemPhys **13**, 9578 (2011).
[39] P. E. Protter, *Stochastic Integration and Differential Equations*, 2nd ed. (Springer, Berlin, 2003).
[40] J. Stockburger and C. H. Mak, J. Chem. Phys. **110**, 4983 (1999).
[41] Y. Tanimura, J. Phys. Soc. Jpn. **75**, 82001 (2006).
[42] W. T. Coffey, Y. P. Kalmykov, and J. T. Waldron, *The Langevin Equation* (World Scientific, Singapore, 1996).
[43] J. M. Noras, Phys. Rev. B **22**, 6474 (1980).